articles

molecular pharmaceutics

Development and Evaluation of a Novel Method for Preclinical Measurement of Tissue Vascular Volume

C. Andrew Boswell,[†] Gregory Z. Ferl,[†] Eduardo E. Mundo,[†] Michelle G. Schweiger,[‡] Jan Marik,[§] Michael P. Reich,[‡] Frank-Peter Theil,[†] Paul J. Fielder,[†] and Leslie A. Khawli*,[†]

Department of Pharmacokinetic and Pharmacodynamic Sciences, Department of Investigative Safety Assessment, and Department of Biomedical Imaging, Genentech Research and Early Development, South San Francisco, California 94080

Received May 28, 2010; Revised Manuscript Received July 16, 2010; Accepted July 26, 2010

Abstract: Identification of clinically predictive models of disposition kinetics for antibody therapeutics is an ongoing pursuit in drug development. To encourage translation of drug candidates from early research to clinical trials, clinical diagnostic agents may be used to characterize antibody disposition in physiologically relevant preclinical models. TechneScan PYP was employed to measure tissue vascular volumes (V_v) in healthy mice. Two methods of red blood cell (RBC) labeling were compared: a direct in vivo method that is analogous to a clinical blood pool imaging protocol, and an indirect method in which radiolabeled blood was transfused from donor mice into recipient mice. The indirect method gave higher precision in RBC labeling yields, lower V_v values in most tissues, and lower ^{99m}Tc uptake in kidneys and bladder by single photon emission computed tomographic (SPECT) imaging relative to the direct method. Furthermore, the relative influence of each method on the calculated area under the first 7 days of the concentration−time curve (AUC_{0-7}) of an IgG in nude mice was assessed using a physiologically based pharmacokinetic model. The model was sensitive to the source of V_v values, whether obtained from the literature or measured by either method, when used to predict experimental AUC_{0-7} values for radiolabeled trastuzumab in healthy murine tissues. In summary, a novel indirect method for preclinical determination of V_v offered higher precision in RBC labeling efficiency and lower renal uptake of ^{99m}Tc than the direct method. In addition, these observations emphasize the importance of obtaining accurate physiological parameter values for modeling antibody uptake.

Keywords: Vascular volume; red blood cell labeling; TechneScan PYP; physiologically based pharmacokinetic modeling

Introduction

Establishing correlations between in vitro, preclinical, and clinical data sets is a prevalent task in drug development that can be complicated by differences in, or absence of, certain physiological processes.[1] For instance, a drug having excellent in vitro potency may fail in preclinical or clinical evaluation due to poor pharmacokinetics (PK). Moreover, differences in PK among various species or strains that originate from physiological variability may, under certain

* To whom correspondence should be addressed. Mailing address: Early Development Pharmacokinetics and Pharmacodynamics, Genentech, Inc., South San Francisco, CA 94080. Telephone: 650-225-6509. Fax: 650-742-5234. E-mail: khawli.leslie@gene.com.

[†] Department of Pharmacokinetic and Pharmacodynamic Sciences.

[‡] Department of Investigative Safety Assessment.

[§] Department of Biomedical Imaging.

(1) Boswell, C. A.; Deng, R.; Lin, K.; Putnam, W. S.; Lei, C.; Theil, F. P.; Joshi, A.; Fielder, P. J.; Khawli, L. A. In vitro-in vivo correlations of pharmacokinetics, pharmacodynamics and metabolism for antibody therapeutics. In *Proteins and Peptides: Pharmacokinetic, Pharmacodynamic, and Metabolic Outcomes*; Mrsny, R. J., Daugherty, A., Eds.; Informa HealthCare: New York, 2009; pp 15−52.

10.1021/mp100183k
Published on Web 07/26/2010

circumstances, be predicted by physiologically based pharmacokinetic (PBPK) modeling. A large amount of physiological data for laboratory animals and humans is reported in the literature;[2−9] however, the manner in which it is utilized should be approached with an understanding of several limitations. The importance of PBPK modeling in enhancing mechanistic understanding of drug kinetics and predicting tissue concentrations of various antibodies currently in development warrants the direct measurement of physiological parameter values whenever possible, to accurately reflect tissue physiological conditions.[10]

Various noninvasive, modern imaging methods are available for preclinical[11−17] and clinical[12,18−23] estimation of vascular volume. For example, vascular volume can be estimated via magnetic resonance (MR) using tracer kinetic models.[24] In contrast, invasive preclinical methods for quantification of blood volume provide direct, presumably more accurate, blood sampling and do not require estimation of parameters.[25−33] In fact, invasive techniques for vascular volume measurement are often used to validate noninvasive

(2) Brown, R. P.; Delp, M. D.; Lindstedt, S. L.; Rhomberg, L. R.; Beliles, R. P. Physiological parameter values for physiologically based pharmacokinetic models. *Toxicol. Ind. Health* **1997**, *13* (4), 407–484.

(3) Davies, B.; Morris, T. Physiological parameters in laboratory animals and humans. *Pharm. Res.* **1993**, *10* (7), 1093–1095.

(4) Baxter, L. T.; Zhu, H.; Mackensen, D. G.; Jain, R. K. Physiologically based pharmacokinetic model for specific and nonspecific monoclonal antibodies and fragments in normal tissues and human tumor xenografts in nude mice. *Cancer Res.* **1994**, *54* (6), 1517–1528.

(5) Baxter, L. T.; Zhu, H.; Mackensen, D. G.; Butler, W. F.; Jain, R. K. Biodistribution of monoclonal antibodies: scale-up from mouse to human using a physiologically based pharmacokinetic model. *Cancer Res.* **1995**, *55* (20), 4611–4622.

(6) Urva, S. R.; Yang, V. C.; Balthasar, J. P. Physiologically based pharmacokinetic model for T84.66: a monoclonal anti-CEA antibody. *J. Pharm. Sci.* **2010**, *99* (3), 1582–1600.

(7) Poulin, P.; Theil, F. P. Prediction of pharmacokinetics prior to in vivo studies. 1. Mechanism-based prediction of volume of distribution. *J. Pharm. Sci.* **2002**, *91* (1), 129–156.

(8) Mordenti, J. Man versus beast: pharmacokinetic scaling in mammals. *J. Pharm. Sci.* **1986**, *75* (11), 1028–1040.

(9) Bjorkman, S.; Wada, D. R.; Stanski, D. R.; Ebling, W. F. Comparative physiological pharmacokinetics of fentanyl and alfentanil in rats and humans based on parametric single-tissue models. *J. Pharmacokinet. Biopharm.* **1994**, *22* (5), 381–410.

(10) Ferl, G. Z.; Wu, A. M.; DiStefano, J. J., 3rd. A predictive model of therapeutic monoclonal antibody dynamics and regulation by the neonatal Fc receptor (FcRn). *Ann. Biomed. Eng.* **2005**, *33* (11), 1640–1652.

(11) Montet, X.; Figueiredo, J. L.; Alencar, H.; Ntziachristos, V.; Mahmood, U.; Weissleder, R. Tomographic fluorescence imaging of tumor vascular volume in mice. *Radiology* **2007**, *242* (3), 751–758.

(12) O'Connor, J. P.; Carano, R. A.; Clamp, A. R.; Ross, J.; Ho, C. C.; Jackson, A.; Parker, G. J.; Rose, C. J.; Peale, F. V.; Friesenhahn, M.; Mitchell, C. L.; Watson, Y.; Roberts, C.; Hope, L.; Cheung, S.; Reslan, H. B.; Go, M. A.; Pacheco, G. J.; Wu, X.; Cao, T. C.; Ross, S.; Buonaccorsi, G. A.; Davies, K.; Hasan, J.; Thornton, P.; del Puerto, O.; Ferrara, N.; van Bruggen, N.; Jayson, G. C. Quantifying antivascular effects of monoclonal antibodies to vascular endothelial growth factor: insights from imaging. *Clin. Cancer Res.* **2009**, *15* (21), 6674–6682.

(13) Weissleder, R.; Cheng, H. C.; Marecos, E.; Kwong, K.; Bogdanov, A., Jr. Non-invasive in vivo mapping of tumour vascular and interstitial volume fractions. *Eur. J. Cancer* **1998**, *34* (9), 1448–1454.

(14) Kim, Y. R.; Rebro, K. J.; Schmainda, K. M. Water exchange and inflow affect the accuracy of T1-GRE blood volume measurements: implications for the evaluation of tumor angiogenesis. *Magn. Reson. Med.* **2002**, *47* (6), 1110–1120.

(15) Bhujwalla, Z. M.; Artemov, D.; Natarajan, K.; Ackerstaff, E.; Solaiyappan, M. Vascular differences detected by MRI for metastatic versus nonmetastatic breast and prostate cancer xenografts. *Neoplasia* **2001**, *3* (2), 143–153.

(16) Henderson, E.; Sykes, J.; Drost, D.; Weinmann, H. J.; Rutt, B. K.; Lee, T. Y. Simultaneous MRI measurement of blood flow, blood volume, and capillary permeability in mammary tumors using two different contrast agents. *Magn. Reson. Imaging* **2000**, *12* (6), 991–1003.

(17) Ter-Pogossian, M. M.; Phelps, M. E.; Grubb, R. L., Jr.; Gado, M. Measure of regional cerebral blood volume in vivo by means of excited fluorescent x-radiation, and factors affecting this parameter. *Eur. Neurol.* **1971**, *6* (1), 218–223.

(18) Laking, G. R.; Price, P. M. Positron emission tomographic imaging of angiogenesis and vascular function. *Br. J. Radiol.* **2003**, *76 Spec No 1* (1), S50–59.

(19) O'Connor, J. P.; Jackson, A.; Parker, G. J.; Jayson, G. C. DCE-MRI biomarkers in the clinical evaluation of antiangiogenic and vascular disrupting agents. *Br. J. Cancer* **2007**, *96* (2), 189–195.

(20) Pavel, D. G.; Zimmer, M.; Patterson, V. N. In vivo labeling of red blood cells with ^{99m}Tc: a new approach to blood pool visualization. *J. Nucl. Med.* **1977**, *18* (3), 305–308.

(21) Atkins, H. L.; Goldman, A. G.; Fairchild, R. G.; Oster, Z. H.; Som, P.; Richards, P.; Meinken, G. E.; Srivastava, S. C. Splenic sequestration of ^{99m}Tc labeled, heat treated red blood cells. *Radiology* **1980**, *136* (2), 501–3.

(22) Smith, T. D.; Richards, P. A simple kit for the preparation of ^{99m}Tc-labeled red blood cells. *J. Nucl. Med.* **1976**, *17* (02), 126–32.

(23) Srivastava, S. C.; Chervu, L. R. Radionuclide-labeled red blood cells: current status and future prospects. *Semin. Nucl. Med.* **1984**, *14* (2), 68–82.

(24) Tofts, P. S. Modeling tracer kinetics in dynamic Gd-DTPA MR imaging. *J. Magn. Reson. Imaging* **1997**, *7* (1), 91–101.

(25) Blumenthal, R. D.; Osorio, L.; Ochakovskaya, R.; Ying, Z.; Goldenberg, D. M. Regulation of tumour drug delivery by blood flow chronobiology. *Eur. J. Cancer* **2000**, *36* (14), 1876–1884.

(26) Gullino, P. M.; Grantham, F. H. The vascular space of growing tumors. *Cancer Res.* **1964**, *24*, 1727–1732.

(27) Sands, H.; Shah, S. A.; Gallagher, B. M. Vascular volume and permeability of human and murine tumors grown in athymic mice. *Cancer Lett* **1985**, *27* (1), 15–21.

(28) Shockley, T. R.; Lin, K.; Sung, C.; Nagy, J. A.; Tompkins, R. G.; Dedrick, R. L.; Dvorak, H. F.; Yarmush, M. L. A quantitative analysis of tumor specific monoclonal antibody uptake by human melanoma xenografts: effects of antibody immunological properties and tumor antigen expression levels. *Cancer Res.* **1992**, *52* (2), 357–366.

(29) Sung, C.; Youle, R. J.; Dedrick, R. L. Pharmacokinetic analysis of immunotoxin uptake in solid tumors: role of plasma kinetics, capillary permeability, and binding. *Cancer Res.* **1990**, *50* (22), 7382–7392.

imaging methods.[17,34] In a retro-translational approach, clinically utilized drugs, including radiopharmaceuticals for noninvasive physiologic imaging,[35] may also serve as probes in invasive preclinical studies. For instance, kit preparations for radiolabeling of red blood cells (RBCs) are useful not only for clinical applications[20−23] but may also enable preclinical blood pool imaging[36,37] and determination of vascular volume in tumors[25,27] and healthy tissues.[25] The direct in vivo method is widely used due to its simplicity and convenience;[20] however, limitations of the direct method have been recognized due to the unavoidable presence of non-RBC-associated radioactivity, leading to development of in vitro[38,39] and modified in vivo[40] techniques.

A major goal in the present work was to accurately measure fractional blood volumes of murine tissues while avoiding the potential inconveniences of some RBC labeling techniques, such as use of a four-way stopcock[40] and centrifugation of labeled RBCs.[38] Specifically, transfusion of whole blood (containing ^{99m}Tc-labeled RBCs) from donor mice to a cohort of recipient mice was performed to reduce the influence of non-RBC-associated radioactivity on V_v measurements relative to the direct method. As such, the present study investigates the relative benefits of two distinct protocols for RBC labeling, and results from both methods were compared with each other and with literature-reported fractional blood volume data. To address the limitations of literature-reported parameters, many of which are assumed nominal values, we sought an additional assessment of blood volume data. Tissue uptake of a non-antigen-specific IgG was predicted by PBPK modeling using vascular volume data that was obtained from the literature and volumes measured by the direct and indirect methods; predicted uptake values were compared with experimental uptake data for trastuzumab, as a representative humanized IgG1 monoclonal antibody, in healthy nude mice.

Materials and Methods

Radiochemistry. Technetium-99 m (^{99m}Tc) pertechnetate was purchased from Covidien Radiopharmacy (South San Francisco, CA) and diluted with sterile normal saline prior to intravenous dosing. TechneScan PYP kits for preparation of ^{99m}Tc pyrophosphate injection were also purchased from Covidien Radiopharmacy and used according to label instructions for the in vivo method of blood pool imaging with the appropriate human-to-mouse scaling.

Carrier-free ^{125}I as sodium iodide in 0.1 M NaOH (pH 12−14) (reductant free) was purchased from PerkinElmer Life and Analytical Sciences, Inc. (Waltham, MA). Sep-Pak Plus C-18 bonded silica cartridges for solid phase extraction were purchased from Waters Corp. (Milford, MA). NAP-5 columns were purchased from GE Healthcare (Piscataway, NJ). Glacial acetic acid and *N*-chlorosuccinimide (NCS) were purchased from Alfa Aesar (Ward Hill, MA). Anhydrous chloroform and acetonitrile were purchased from VWR International, LLC (Brisbane, CA). Synthesis of *N*-succinimidyl 3-(tri-*n*-butylstannyl)benzoate (STB) was performed according to reported literature methods.[41] Synthesis and purification of ^{125}I-iodobenzoate (^{125}I-SIB) were achieved through modification of literature-reported procedures.[42−44] Selection of ^{125}I-SIB as a probe, instead of direct radioha-

(30) van Schaijk, F. G.; Oosterwijk, E.; Molkenboer-Kuenen, J. D.; Soede, A. C.; McBride, B. J.; Goldenberg, D. M.; Oyen, W. J.; Corstens, F. H.; Boerman, O. C. Pretargeting with bispecific anti-renal cell carcinoma x anti-DTPA(In) antibody in 3 RCC models. *J. Nucl. Med.* **2005**, *46* (3), 495–501.
(31) Lockman, P. R.; McAfee, G.; Geldenhuys, W. J.; Van der Schyf, C. J.; Abbruscato, T. J.; Allen, D. D. Brain uptake kinetics of nicotine and cotinine after chronic nicotine exposure. *J Pharmacol. Exp. Ther.* **2005**, *314* (2), 636–642.
(32) Park, S.; Sinko, P. J. P-glycoprotein and multidrug resistance-associated proteins limit the brain uptake of saquinavir in mice. *J. Pharmacol. Exp. Ther.* **2005**, *312* (3), 1249–1256.
(33) O'Connor, S. W.; Bale, W. F. Accessibility of circulating immunoglobulin G to the extravascular compartment of solid rat tumors. *Cancer Res.* **1984**, *44* (9), 3719–3723.
(34) Ferrier, M. C.; Sarin, H.; Fung, S. H.; Schatlo, B.; Pluta, R. M.; Gupta, S. N.; Choyke, P. L.; Oldfield, E. H.; Thomasson, D.; Butman, J. A. Validation of dynamic contrast-enhanced magnetic resonance imaging-derived vascular permeability measurements using quantitative autoradiography in the RG2 rat brain tumor model. *Neoplasia* **2007**, *9* (7), 546–555.
(35) Boswell, C. A.; Bumbaca, D.; Pastuskovas, C. V.; Mundo, E. E.; Shen, B. Q.; Carano, R. A. D.; Marik, J.; Williams, S. P.; Theil, F. P.; Fielder, P. J.; van Bruggen, N.; Khawli, L. A. Molecular imaging in cancer drug development. In *Molecular imaging probes for cancer research*, 1st ed.; Chen, X., Ed. World Scientific: Hackensack, NJ, 2010; in press.
(36) Vanhove, C.; Lahoutte, T.; Defrise, M.; Bossuyt, A.; Franken, P. R. Reproducibility of left ventricular volume and ejection fraction measurements in rat using pinhole gated SPECT. *Eur. J. Nucl. Med. Mol. Imaging* **2005**, *32* (2), 211–220.
(37) Chin, B. B.; Metzler, S. D.; Lemaire, A.; Curcio, A.; Vemulapalli, S.; Greer, K. L.; Petry, N. A.; Turkington, T. G.; Coleman, R. E.; Rockman, H.; Jaszczak, R. J. Left ventricular functional assessment in mice: feasibility of high spatial and temporal resolution ECG-gated blood pool SPECT. *Radiology* **2007**, *245* (2), 440–448.
(38) Neumann, P.; Schicha, H.; Schurnbrand, P.; Bahre, M.; Emrich, D. Visualizing cardiac blood pool: comparison of three labeling methods. *Eur. J. Nucl. Med.* **1983**, *8* (11), 463–466.
(39) Patrick, S. T.; Glowniak, J. V.; Turner, F. E.; Robbins, M. S.; Wolfangel, R. G. Comparison of in vitro RBC labeling with the UltraTag RBC kit versus in vivo labeling. *J. Nucl. Med.* **1991**, *32* (2), 242–244.
(40) Callahan, R. J.; Froelich, J. W.; McKusick, K. A.; Leppo, J.; Strauss, H. W. A modified method for the in vivo labeling of red blood cells with Tc-99m: concise communication. *J. Nucl. Med.* **1982**, *23* (4), 315–318.
(41) Vaidyanathan, G.; Zalutsky, M. R. Preparation of *N*-succinimidyl 3-[*I]iodobenzoate: an agent for the indirect radioiodination of proteins. *Nat. Protoc.* **2006**, *1* (2), 707–713.
(42) Wang, L. H.; Wang, Y. X.; Yin, D. Z.; Li, J. L. Radioiodination of aromatic organostannates. *J. Radioanal. Nucl. Chem.* **2003**, *258* (3), 685–688.
(43) Matloobi, M.; Rafii, H.; Beigi, D.; Khalaj, A.; Kamali-Dehghan, M. Synthesis of radioiodinated labeled peptides. *J Radioanal. Nucl. Chem.* **2003**, *257* (1), 71–73.

logenation, ensured that the level of radioactivity in tissues and blood would reflect the true PK of the antibody as much as possible. Indirect iodination avoids exposure of proteins to oxidizing conditions during radiolabeling and produces radioimmunoconjugates that are less susceptible to enzymatic deiodination in vivo.[41]

Solutions of STB, 0.1 mg/mL in 0.5% acetic acid/chloroform, and NCS, 25 mg/mL in chloroform, were freshly prepared and stored in darkness at 4 °C until use. The following reagents were sequentially added to a glass vial: 2 μL of 0.1 mg/mL STB in 0.5% acetic acid/chloroform, 100 μL of 0.5 M acetic acid in chloroform, 5 μL (59.2 MBq) of sodium [^{125}I]iodide in 0.1 M NaOH (pH 12−14), and 10 uL of 25 mg/mL *N*-chlorosuccinimide in chloroform. The reaction mixture was thoroughly vortexed followed by agitation at 550 rpm for 10 min at 20 °C. Rapid solvent removal was facilitated by a gentle stream of N_2 gas (<1 min), and the resulting residue was dissolved in a 5 mL aliquot of 0.1% acetic acid in sterile deionized H_2O. A C-18 Sep-Pak Plus cartridge was activated with 5 mL of acetonitrile, followed by 5 mL of 0.1% acetic acid in sterile deionized H_2O. The entire reaction mixture was loaded onto the primed Sep-Pak cartridge, followed by three 5 mL washes of the same aqueous acidic solution, and three 5 mL volumes of air to expel excess water. The radioactive retentate, ^{125}I-SIB, was eluted with minimal (≤1 mL) anhydrous acetonitrile. The reverse-phase solid-phase extraction (SPE) procedure outlined above was necessary to remove excess oxidant, not radioactive impurities.

Subsequent to removal of solvent from ^{125}I-SIB under vacuum, a 4.0 μL (84 μg) aliquot of the concentrated antibody (21 mg/mL trastuzumab) in phosphate-buffered saline (PBS) was added directly to the tube, followed by a complementary volume of 0.05 M borate buffer (pH 8.5) such that the total reaction volume was 50 μL. The reaction mixture was incubated at 37 °C for 45 min. Meanwhile, a NAP-5 column was equilibrated with at least three column volumes of PBS. The reaction mixture was diluted with 50 μL of PBS, and the resulting 100 μL sample was loaded onto the NAP-5 column and allowed to settle by gravity, followed by an additional 400 μL of PBS. Once this volume settled into the column, the ^{125}I-SIB-labeled antibody product was eluted into a clean collection tube by applying an additional 600 μL of PBS to the column. Purity of the radioimmunoconjugate was assessed by size-exclusion radio-HPLC (isocratic, PBS, 0.5 mL/min) on an Agilent 1100 series HPLC system operated through ChemStation software and equipped with a Biosep-SEC-S 3000 column (Phenomenex) and a Raytest Ramona 90 radioactive flow monitor.

Animal Model. The protocol, housing, and anesthesia were approved by the Institutional Animal Care and Use Committees (IACUC) of Genentech Laboratory Animal Resources (LAR), in compliance with AAALAC (Association for Assessment and Accreditation of Laboratory Animal Care) regulations. Female beige nude XID (bg.nu.xid Harlan) mice in a 6−8-week age range were used for all measurements.

Vascular Volume. The intravascular spaces of murine tissues were measured by ^{99m}Tc labeling of RBCs in vivo following administration of stannous (Sn^{2+}) pyrophosphate.[20,25,45,46] Use of the clinical TechneScan PYP kit is conceptually based on the original method of Sands for in situ (i.e., in vivo) RBC labeling with ^{99m}Tc.[25,27,47] The previous administration of stannous pyrophosphate, a component of the reconstituted TechneScan kit, has been postulated to reduce ^{99m}Tc pertechnetate intracellularly so that it may bind to the beta chain of hemoglobin.[48] However, this process is highly dependent on labeling conditions,[49] with the additional possibility of a significant portion of cytoplasmic or cell-surface-associated ^{99m}Tc.[49,50]

Immediately before injection, the kit vial was allowed to warm to 25 °C, reconstituted with 3 mL of normal sterile nonpyrogenic saline containing no preservatives, thoroughly vortexed, and visually inspected for particulate matter. Each clinical vial contains 4 mg of tin chloride (3 human doses) in 3000 μL, while a preclinical dose of only 0.5 μg of tin chloride is desired assuming a 70 kg human and 0.02 kg mouse. A 37.5 μL (50 μg) aliquot of this solution was removed, diluted to 10 mL of saline, and mixed; 100 μL doses were promptly drawn from this solution.

Direct in Vivo RBC Labeling (i.e., Direct Method). An intravenous bolus dose of reconstituted TechneScan PYP was followed exactly 30 min later by a 555-kBq intravenous bolus dose of ^{99m}Tc pertechnetate. One hour later, blood and tissue samples were collected by retro-orbital bleed and terminal organ harvest, respectively, and counted for radioactivity expressed in counts per minute (CPM) in the appropriate

(44) Khawli, L. A.; Kassis, A. I. Synthesis of ^{125}I labeled *N*-succinimidyl *p*-iodobenzoate for use in radiolabeling antibodies. *Int. J. Rad. Appl. Instrum. B* **1989**, *16* (7), 727–733.

(45) LeBerthon, B.; Khawli, L. A.; Alauddin, M.; Miller, G. K.; Charak, B. S.; Mazumder, A.; Epstein, A. L. Enhanced tumor uptake of macromolecules induced by a novel vasoactive interleukin 2 immunoconjugate. *Cancer Res.* **1991**, *51* (10), 2694–2698.

(46) Khawli, L. A.; Miller, G. K.; Epstein, A. L. Effect of seven new vasoactive immunoconjugates on the enhancement of monoclonal antibody uptake in tumors. *Cancer* **1994**, *73* (3), 824–831.

(47) Sands, H.; Jones, P. L.; Shah, S. A.; Palme, D.; Vessella, R. L.; Gallagher, B. M. Correlation of vascular permeability and blood flow with monoclonal antibody uptake by human Clouser and renal cell xenografts. *Cancer Res.* **1988**, *48* (1), 188–193.

(48) Rehani, M. M.; Sharma, S. K. Site of Tc-99m binding to the red blood cell: concise communication. *J. Nucl. Med.* **1980**, *21* (7), 676–678.

(49) Mariani, G.; Pauwels, E. K.; AlSharif, A.; Marchi, S.; Boni, G.; Barreca, M.; Bellini, M.; Grosso, M.; de Bortoli, N.; Mumolo, G.; Costa, F.; Rubello, D.; Strauss, H. W. Radionuclide evaluation of the lower gastrointestinal tract. *J. Nucl. Med.* **2008**, *49* (5), 776–787.

(50) Seldin, D. W.; Simchon, S.; Jan, K. M.; Chien, S.; Alderson, P. O. Dependence of technetium-99m red blood cell labeling efficiency on red cell surface charge. *J. Nucl. Med.* **1988**, *29* (10), 1710–1713.

gamma energy window. Vascular volume (V_v) was calculated as (CPM of ^{99m}Tc in 1 g of tissue)/(CPM of ^{99m}Tc in 1 μL of blood).

Indirect in Vivo RBC Labeling (i.e., Transfusion Method). Two mice each received an intravenous bolus dose of reconstituted TechneScan PYP followed exactly 30 min later by a 5550-kBq intravenous bolus dose of ^{99m}Tc pertechnetate. One hour later, both mice were sacrificed by exsanguination while collecting blood into EDTA-coated tubes. The radiolabeled whole blood was pooled, an aliquot was removed for processing into plasma and pellet by centrifugation, and 150 μL doses were gently drawn and promptly administered to naïve mice (i.e., no tinning of the blood was necessary). Mice were sacrificed 1 h later, with organ harvest and analysis performed exactly as described for direct RBC labeling.

SPECT-CT Imaging. Single photon emission computed tomography/X-ray computed tomography (SPECT-CT) imaging of mice with ^{99m}Tc-labeled RBCs was performed as an adjunct to the ex vivo biodistribution studies on an X-SPECT SPECT-CT scanner (Gamma-Medica, Northridge, CA) equipped with a dual gamma camera SPECT system and X-ray cone beam CT scanner. Quantitative data were not derived from the images. The X-SPECT uses a pair of 80 × 80 pixel gamma cameras and is equipped with position sensitive photomultiplier tubes coupled to NaI(Tl) scintillators. The high-resolution, low-energy multipinhole collimator (5B10) used in this study was designed for imaging of mice and has the following specifications: 1.0 mm hole diameter, 5 pinholes, 75 mm focal length, and 65° acceptance angle. The CT scanner has a 2368 × 2240 pixel complementary metal-oxide-semiconductor (CMOS) X-ray detector, 50 μm pixel pitch, an X-ray source with a focal spot size of 75 μm, and a 9.7 cm (axial) × 9.3 cm (transaxial diameter) cylindrical field of view.

Red blood cell labeling was performed exactly as described for the invasive, nonimaging arm of the study (see Vascular Volume section) except for the use of higher amounts of radioactivity. All mice received a bolus intravenous dose consisting of ^{99m}Tc pertechnetate in 100 μL of saline or a 200 μL aliquot of ^{99m}Tc-labeled whole blood, with total injected radioactivity in the range of 23.5−27.4 MBq. Initiation of SPECT-CT imaging was executed at 98−106 min from the time of tracer injection. Image acquisition times for CT and SPECT were an average of 3 and 12 min, respectively, with approximately 20 000 counts per projection (20 s per projection) for the latter. Mice were placed in a prone position on the bed and maintained under anesthesia with sevoflurane, which was delivered using a precision vaporizer (VetEquip, Pleasanton, CA). Sevoflurane has been previously demonstrated as superior to isoflurane for physiologic imaging in mice.[51] Images were acquired using the above-mentioned CT and γ-ray detectors sequentially without removing the mouse from the gantry. During CT image acquisition, the X-ray tube was operated at 75 kVp with 0.3 mA current. Images were captured for 250 ms per view for 256 views in 360° rotation. Immediately after CT acquisition, SPECT images were acquired on the 140 keV photopeak of ^{99m}Tc with a −5 to +10% window using a high-resolution 5-pinhole collimator and a 4.5 cm radius of rotation. The tomographic acquisition protocol of the LumaGEM software provided with the X-SPECT was used. Mice were subsequently euthanized under sedation, and tissues collected for gamma counting in a manner identical to that used for the nonimaging arm of the study. The SPECT and CT data was transformed to a 256 × 256 matrix and fused using AMIRA graphics software (TGS, San Diego, CA), allowing the achievement of simultaneous scintigraphic and anatomic information in all tomographic scans in the three different spatial axes.

PK and Tissue Distribution. Dosing solutions were prepared by mixing ^{125}I-SIB-trastuzumab with nonradiolabeled trastuzumab to achieve a total protein dose of exactly 10 mg/kg and a radioactive dose of approximately 14.8 MBq/kg in no more than 100 μL of PBS. Mice received a single bolus dose via tail vein injection. A 50 μL aliquot of EDTA whole blood was terminally collected at 4 h, 1 day, 3 days, 7 days, and 14 days via cardiac puncture under inhaled isoflurane anesthesia. Additional 50 μL EDTA whole blood samples were collected nonterminally at 5 min, 2 h, 6 h, 48 h, 96 h, 216 h, and 264 h via retro-orbital bleed under inhaled isoflurane anesthesia. The following tissues were terminally harvested: liver, spleen, kidneys, lungs, heart, gastrocnemius muscle, and mammary fat pad. All tissues were rinsed with PBS, blot dried, weighed, frozen on dry ice, and stored at −70 °C. Blood, tissues, and 5 μL aliquots of dosing solution standards were counted for radioactivity using a 1480 WIZARD gamma counter (Wallac, Turku, Finland) in the energy window for the 29 keV photon peak of ^{125}I with automatic background and decay correction. Counts per minute (CPM) were converted to percentage of injected dose per gram (%ID/g) of blood or tissue. For tissues, %ID/g values were transferred to GraphPad Prism 5.03, and the areas under the first 7 days of the concentration−time curve (AUC_{0-7}) values were calculated using the trapezoidal rule assuming no uptake at time zero. Standard deviations (σ) for AUC_{0-7} values were computed from the σ in tissue concentration at individual time points using a previously reported approach.[52] The time range of 0−7 days for AUC calculation was chosen since the PBPK model was calibrated using mAb PK data collected for 1 week.[10] For blood, a sum of two exponentials was fitted to all data through 14 days using GraphPad Prism 5.03 in order to estimate the %ID/g value immediately after dosing; AUC_{0-7} for blood was subsequently calculated using this extrapolated value.

(51) Flores, J. E.; McFarland, L. M.; Vanderbilt, A.; Ogasawara, A. K.; Williams, S. P. The effects of anesthetic agent and carrier gas on blood glucose and tissue uptake in mice undergoing dynamic FDG-PET imaging: sevoflurane and isoflurane compared in air and in oxygen. *Mol. Imaging Biol.* **2008**, *10* (4), 192–200.

(52) Bailer, A. J. Testing for the equality of area under the curves when using destructive measurement techniques. *J. Pharmacokinet. Biopharm.* **1988**, *16* (3), 303–309.

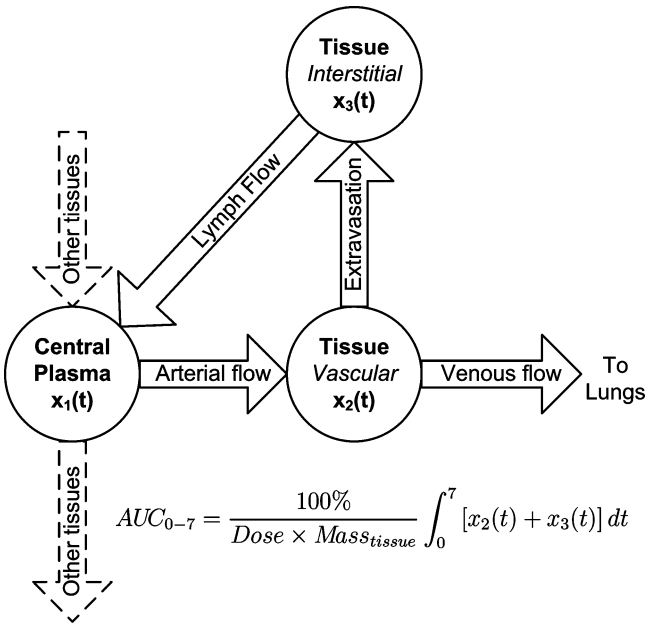

Figure 1. Typical tissue submodel component of the physiologically based pharmacokinetic model.[10] Antibody enters tissue from the central plasma compartment via arterial blood flow where it continues to the lungs via venous blood flow or returns directly to the central plasma compartment through the lymphatic system subsequent to extravasation into interstitial space. The AUC_{0-7} values listed in Table 2 are the sum of AUCs of absolute antibody amount vs time in the two tissue compartments (x_2 and x_3) multiplied by 100% and divided by the product of the dose and total mass of tissue, yielding AUC units of %ID/g × time. Note that the muscle submodel includes extra compartments, included in the AUC_{0-7} calculation, that describe FcRn mediated recycling and degradation of antibody.

PBPK Simulations. In order to assess the potential impact of parameter variability on physiologically based modeling results, organ level monoclonal antibody (mAb) biodistribution was simulated using a previously published PBPK model[10] that accounts for FcRn mediated rescue of IgG from degradation (Figure 1). The areas under the first 7 days of the concentration−time curve (AUC_{0-7}) for blood and selected tissues were calculated using parameter values taken from the literature as well as with the experimentally measured values discussed herein (Table 1). Note that the literature V_v values in Table 1 were derived from reported fractional blood volumes (γ, where $\gamma = V_v/V_{tissue}$) by assuming a tissue density of 1 g/mL, consistent with assumptions made in the reference from which they were obtained.[4] A comparison was made between AUC_{0-7} calculated using literature versus experimentally measured blood volumes by substituting literature values of V_v with values measured using the direct ($V_{v,Direct}$) and indirect ($V_{v,Indirect}$) RBC labeling methods.

Results

Radiochemistry. An overall 50% radiochemical yield of ^{125}I-SIB-trastuzumab was achieved, with an initial 55.5-MBq aliquot of ^{125}I yielding approximately 29.6 MBq of product at a specific activity of approximately 350 MBq/mg. Accuracy of yield calculations may have been affected by noticeable geometric effects in dose calibration measurements. Greater than 95% radiochemical purity was evident by size-exclusion radiochromatography.

Table 1. Comparison of Measured Tissue Vascular Volumes (V_v) in Normal, Naïve Mice ($n = 5$) to Literature-Reported Values[a]

tissue	literature	V_v, direct method	V_v, indirect method
brain	9.4[b,e]	11.0 ± 1.95	10.8 ± 1.61
spleen	100[c,f]	149 ± 20.8	121 ± 29.4
liver	100[c,f]	193 ± 33.7	42.0 ± 7.71[i]
kidney	100[c,f]	428 ± 117	77.5 ± 7.25[i]
ileum	29[c,g]	22.3 ± 11.6	7.52 ± 2.42[i]
heart	52.6[c,g]	45.0 ± 5.27	29.9 ± 6.59[i]
lung	100[c,f]	216 ± 46.0	235 ± 111
muscle	18.9[c,g]	15.4 ± 6.29	8.72 ± 1.98
fat	20[d,h]	61.4 ± 29.6	14.2 ± 4.28[i]

[a] All values are reported in μL/g. Note that the assay method can greatly influence measured V_v, especially in probe clearance organs. [b] Reference 32. [c] Reference 4. [d] Reference 2. [e] Measured using ^{3}H-inulin. [f] For well-perfused organs, 10% vascular space is assumed.[4] [g] Estimated based on experimental data (IgG in plasma, tissues) at early time points.[4] [h] Estimated from human data. [i] Statistically significant difference by unpaired *t*-test ($P < 0.05$).

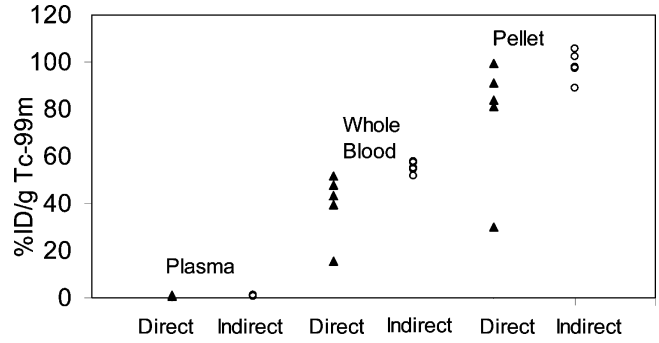

Figure 2. Percentage of the injected dose of ^{99m}Tc per gram of tissue (%ID/g) ($n = 5$) using the direct (solid triangles) and indirect (open circles) in vivo RBC labeling methods in female beige nude mice. For the direct method, these values represent the in vivo red blood cell (RBC) labeling yield. In contrast, the indirect method involves injection of whole blood containing RBCs that were previously labeled in donor mice.

Vascular Volume. The portion of RBC-associated radioactivity in blood collected from donor mice was found to be >98%; this was verified by cell fractionation of sampled aliquots of pooled whole blood containing radiolabeled RBCs prior to injection into recipient mice for indirect V_v measurement. Successful RBC labeling with ^{99m}Tc was evident due to the vast majority of radioactivity being associated with the RBC pellet fraction independent of the method used (Figure 2). Specifically, the %ID/g values for the direct and indirect methods, respectively, were 0.79 ± 0.14 vs 0.63 ± 0.19 in plasma, 39.6 ± 14.2 vs 55.1 ± 2.5 in whole blood, and 77.1 ± 27.3 vs 98.3 ± 6.2 in the RBC pellet. As

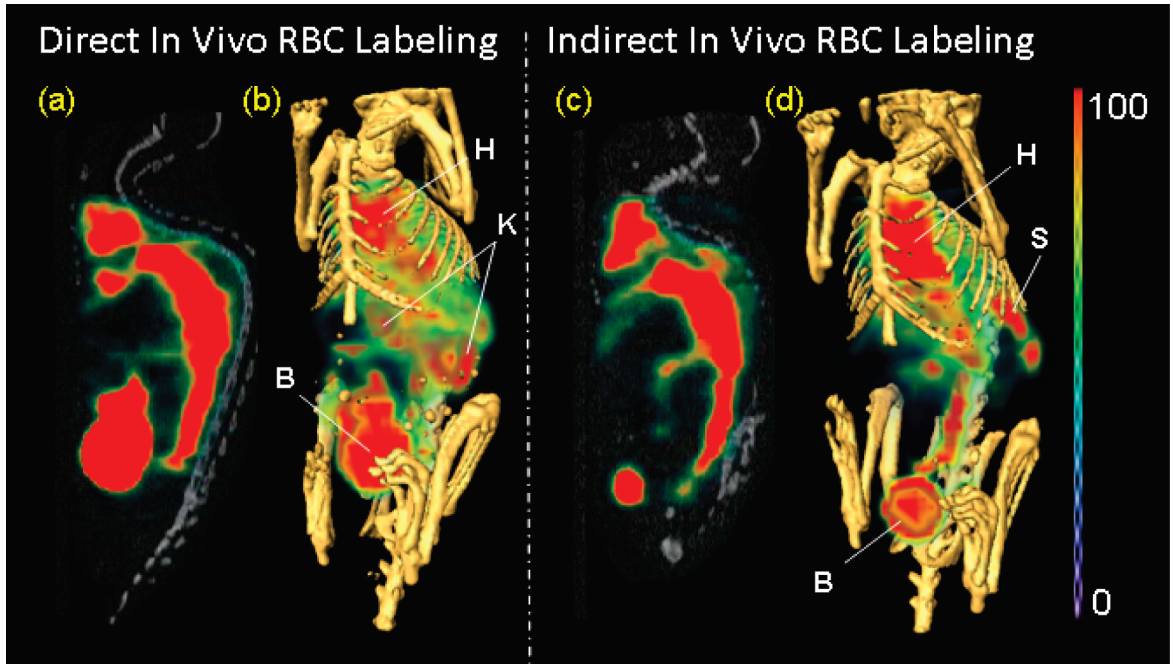

Figure 3. Representative SPECT-CT images ($n = 1$) obtained at 98−106 min post injection of female beige nude mice following RBC labeling by the direct (a, b) and indirect (c, d) methods. The false-colored SPECT images in arbitrary uptake units are fused onto the X-ray CT images. Both a two-dimensional sagittal slice along the spinal plane (a, c) and a corresponding three-dimensional volume rendering (b, d) are shown for each reconstructed SPECT-CT fusion image. Mostly blood pool and bladder uptake are evident in the sagittal slices. The locations of visible uptake in heart (H), kidneys (K), spleen (S), and bladder (B) are indicated in the volume rendering images.

expected, %ID/g values for whole blood were roughly half of those for the RBC pellet based on a typical hematocrit value of 45% in mice.[3] Higher precision in labeling efficiency for the indirect method was apparent, with coefficients of variation (CV) in %ID/g values for the direct and indirect methods, respectively, as follows: 36 and 5% in blood, 35 and 6% in RBC pellet. The trend was maintained even when a single mouse outlier (Figure 2) was omitted, yielding CV values of 12 and 9% for the direct method in blood and RBC pellet, respectively.

Mean values with standard deviations were calculated for V_v data produced by both methods and compared with literature values (Table 1). The indirect method gave a lower average V_v value than the direct method for several tissues (Table 1). Percent differences, expressed as $[(V_{v,Direct} - V_{v,Indirect})/V_{v,Direct}] \times 100\%$, were as follows: 19% in spleen, 34% in heart, 9% (increase) in lung, 43% in muscle, 78% in liver, 82% in kidney, 66% in ileum, and 77% in fat. By conventional criteria ($P < 0.05$), these differences were statistically significant by unpaired t-test for liver, kidneys, heart, fat, and ileum, but not for muscle, brain, spleen, and lungs. The $V_{v,Indirect}$ value for kidneys (77.5 ± 7.25 μL/g) showed a much closer agreement to the literature reported value (100 μL/g) than the $V_{v,Direct}$ value (428 ± 117 μL/g) (Table 1). This discrepancy may be explained by renal clearance of a fraction of ^{99m}Tc that did not become associated with RBCs. In many organs, the indirect method also gave substantially lower V_v values than the literature reported values (Table 1). The origin of values reported in the literature should be carefully considered, as many are in fact assumed nominal values: for instance, a 10% vascular space is assumed for well-perfused organs (e.g., kidney, lung, liver, and spleen), while other values are estimated based on experimental uptake data of antibodies at early time points.[4]

SPECT-CT Imaging. The differences in whole-body distribution between the two methods were also visually assessed by SPECT-CT imaging. While the sagittal two-dimensional slices (a, c) revealed similar blood distribution images for both methods, the three-dimensional volume renderings (b, d) demonstrated lower uptake for the indirect RBC labeling method, especially in kidneys and bladder (Figure 3). It should be noted that the peak in renal uptake for the direct method may not have been completely captured by imaging due to the longer time (98−106 min) between injection and the start of SPECT data acquisition; in contrast, mice that were used to generate the data in Figure 2 and Table 1 were promptly sacrificed at 1 h post-injection of ^{99m}Tc. Slight splenic uptake was also evident in the SPECT-CT volume rendered images; this is expected due to the spleen's physiological role in sequestration of RBCs.[21−23] Invasive tissue distribution was also performed immediately after noninvasive imaging; calculated V_v for all tissues from the imaging mice (data not shown) agreed well with the data in Table 1.

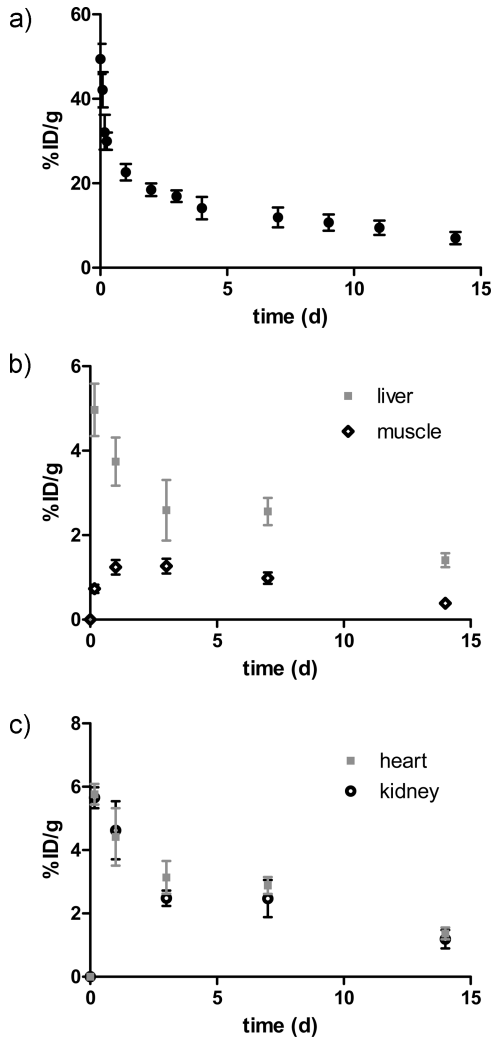

Figure 4. Blood pharmacokinetic profile (a) and selected tissue distribution (b, c) data (%ID/g) for ^{125}I-SIB-trastuzumab (10 mg/kg) in healthy female beige nude mice. Muscle samples originated from the gastrocnemius.

PK and Tissue Distribution. An elimination half-life of 8 days was obtained from the biexponential blood PK curve of ^{125}I-SIB-trastuzumab (Figure 4a). The tissue distribution trend in blood-rich organs (e.g., liver, kidney, heart) generally reflected blood PK with a continuous decrease over time (Figure 4b, c). Spleen and lung followed a similar trend (data not shown). In contrast, relatively blood-poor tissues (e.g., muscle) demonstrated an initial increase in uptake, peaking at 1−3 days, followed by slow clearance (Figure 4b). The mammary fat pad followed a similar trend (data not shown). Values of %ID/g from 4 h to 14 days ranged from 32 ± 4 to 7.0 ± 1.5 for blood, 5.0 ± 0.6 to 1.4 ± 0.2 for liver, 7.2 ± 2.5 to 1.8 ± 1.0 for spleen, 5.7 ± 0.3 to 1.2 ± 0.3 for kidneys, 6.0 ± 1.2 to 2.0 ± 0.3 for lungs, 5.8 ± 0.3 to 1.4 ± 0.2 for heart, 1.3 ± 0.2 to 0.39 ± 0.03 for muscle, and 3.0 ± 0.5 to 0.72 ± 0.15 for mammary fat pad (Figure 4). From these data, the experimentally determined AUC_{0-7} values in Table 2 were generated.

Table 2. Comparison of Model-Predicted[10] and Experimentally Measured AUCs [%ID/g × day], up to 7 Days Post-Injection (AUC_{0-7}), Calculated for an Intact mAb in Mice Using Measured and Literature Vascular Volume (V_v) Values[a]

tissue	model-predicted (literature)	model-predicted (direct method)	model-predicted (indirect method)	experimental (^{125}I-SIB-trastuzumab)
blood	82.5	84.0	94.4	122 ± 4.07
liver	18.1	30.5	12.2	20.7 ± 1.38
kidneys	18.7	61.4	18.1	21.8 ± 1.10
spleen	15.4	22.0	20.7	28.1 ± 3.46
lung	36.7	52.3	61.6	33.1 ± 3.04
heart	17.4	16.7	16.7	24.3 ± 1.21
muscle	11.4	9.77	7.89	7.90 ± 0.370
GI	7.03	6.25	4.98	na
bone	7.58	7.72	8.67	na

[a] Experimental AUC values were calculated from mean uptake values ($n = 3$); see Figure 4 for selected data.

PBPK Simulations. Listed in Table 2 are the AUC_{0-7} values for blood and various tissues calculated using both literature values of V_v and experimental values that were measured using the direct and indirect RBC labeling methods. $V_{v,Direct}$ values yield blood and bone AUCs that are 2% higher than those obtained using literature values, while spleen and lung are both 43% higher. Liver and kidneys are 69 and 228% higher while GI is 11% lower. $V_{v,Indirect}$ values yield AUCs for blood and bone that are 14% higher and liver and GI values that are approximately 30% lower when using measured compared with literature parameter values. Spleen and lung are 34 and 68% higher while kidneys are 3% lower. Note that no bone specific measurements were made in this study. Literature values were used for this tissue in all cases, and changes in bone reflect altered blood PK profiles.

Discussion

The original rationale for developing the indirect labeling method was to minimize the influence of non-RBC-associated $^{99m}TcO_4^-$ on V_v measurement. Because the direct method involves injection of free ^{99m}Tc pertechnetate, competition for radioactivity exists between RBCs and the thyroid, stomach, salivary glands, and interstitial fluid spaces of various tissues.[40] Collection and reinjection of in vivo labeled ^{99m}Tc-whole blood from donor mice into recipient mice was performed in expectation that the majority of non-RBC-associated $^{99m}TcO_4^-$ would be sequestered in the carcasses and excreta of donor mice, serving as an "in vivo purification" system. This goal was attained, as strongly evidenced by the indirect method yielding values for %ID/g in the RBC pellet that were higher in magnitude but with lower statistical deviation (Figure 2). Consistent with this observation, lower V_v values (and hence lower $^{99m}TcO_4^-$ uptake) was observed in hepatobiliary organs (liver, ileum) and in organs involved in renal clearance (kidneys, bladder) of $^{99m}TcO_4^-$ (Table 1, Figure 3). The higher uptake in gut may be rationalized by

emptying of stomach contents, as gastric uptake of $^{99m}TcO_4^-$ is known to be mediated by the sodium-iodide symporter.

An additional major advantage of the indirect RBC labeling method is that it reduces interanimal variability by allowing the injection of radiolabeled blood pooled from donor mice. This essentially ensures that the labeling efficiency of RBCs for all study mice is identical, which is not the case for the direct method. Note the markedly reduced statistical variability in RBC labeling efficiency for mice subjected to the indirect method relative to the direct method (Figure 2). The likely cause of the most obvious single mouse outlier is a partial subcutaneous delivery of stannous pyrophosphate and/or ^{99m}Tc; the risk of such interanimal variability is reduced in the indirect method, which involves only a single injection of a homogeneous pool of prelabeled whole blood in each study mouse. In contrast, the direct method requires twice the number of injections (stannous pyrophosphate and ^{99m}Tc), significantly increasing the likelihood of an unsuccessful tail vein injection in any given study animal; indeed, these disadvantages have been noted by others.[53] Furthermore, the administration of certain drugs may potentially alter vascular permeability and/or perfusion, which, in turn, may affect RBC labeling by changing the exposure of cells to stannous ion and/or ^{99m}Tc pertechnetate. The indirect method would be preferred in such cases, since the RBC labeling could be performed in naïve mice.

The intent of the analysis herein is to facilitate a better understanding of physiological parameter data, while providing the reader an appreciation of the various methodologies behind measuring physiological quantities such as tissue vascular volume, thus achieving an awareness of their limitations, especially in regards to organs involved in renal and hepatobiliary clearance. The use of tabular physiological parameter data from a single, well-referenced source is appealing due to convenience and peer acceptance; in this context, an effort was made to select literature values (Table 1) from sources that are heavily cited in numerous PBPK modeling efforts. However, for any single physiological parameter, there is significant variability in values reported by various sources; this discrepancy is often caused by differences in experimental methodology. Parameters such as fractional blood volume vary across species, age, breed, disease state, drug treatment, and time of day,[25] hence justifying direct measurement whenever possible.[54] For some modeling and simulation applications, approximations of physiological parameter values may suffice. However, those who utilize such information should be aware of the methods used to derive the physiological parameter values so that limitations, with respect to accuracy of PBPK model predictions, are known. Unfortunately, the methods used to derive physiological parameter values are often omitted in tables containing compiled data; thus, it is critical to access the original literature source.

Importantly, sensitivity analysis of a previously reported PBPK model implicated vascular volume as one of the most influential parameters on antibody concentration in tissues, particularly at early time points.[4] Comparing PBPK modeling results based on literature and measured physiological parameter values demonstrates the importance of obtaining accurate estimates for use with the model. While the change in blood AUC is modest (2−14%) (Table 2), the impact of using measured physiological values is potentially high when simulating concentration−time curves within clearance organs, with changes in liver and kidney AUCs ranging from 33 to 69% and 3 to 228%, respectively, depending on the source of the parameter values. Variability in AUC_{0-7} for liver is of particular significance when modeling mAb biodistribution. The range of AUC_{0-7} values for kidney (Table 2) can be rationalized by the superiority of the novel indirect in vivo RBC labeling technique over the traditional direct in vivo method. Direct RBC labeling is not appropriate for measurement of renal V_v due to clearance of the portion of ^{99m}Tc pertechnetate that is not sequestered by the tinned RBCs. This artifact was largely avoided in the indirect method by performing the RBC labeling in donor mice and transfusing the labeled blood into study mice, resulting in noticeably lower uptake in bladder and kidneys by SPECT-CT (Figure 3) and lower uptake in liver, kidney, ileum, and fat by invasive tissue distribution (Table 1).

Two distinct labeling methods were assessed in this work to determine their relative strengths and weaknesses in measuring the physiological parameter, V_v. Radiolabeling of RBCs is a common method for both preclinical[36,37] and clinical[20−23] blood pool imaging and for determination of V_v in tumors[25,27] and normal tissues.[25] While in vitro labeling and subsequent injection of RBCs is possible, methods have been developed for in vivo labeling using stannous chloride as a reducing agent.[27] Commercialized clinical kits (i.e., TechneScan PYP) are now available for this purpose and can be scaled down for preclinical use. The V_v results in the present study suggest that transfusion of labeled RBCs gives a more physiologically relevant measurement of V_v in such tissues by avoiding nonspecific uptake of ^{99m}Tc. Low levels of plasma-associated ^{99m}Tc (<1% ID/g) were obtained for both methods; however, this does not account for the fraction of pertechnetate distributing to the interstitial fluid compartment.[40] This new indirect in vivo methodology is also applicable to noninvasive imaging; this was demonstrated by the feasibility of SPECT-CT imaging (Figure 3).

In conclusion, a newly developed indirect RBC labeling method for preclinical tissue vascular volume measurements was designed to reduce the amount of non-RBC-associated ^{99m}Tc; this was accomplished by transfusing radiolabeled

(53) Thrall, J. H.; Freitas, J. E.; Swanson, D.; Rogers, W. L.; Clare, J. M.; Brown, M. L.; Pitt, B. Clinical comparison of cardiac blood pool visualization with technetium-99m red blood cells labeled in vivo and with technetium-99m human serum albumin. *J. Nucl. Med.* **1978**, *19* (7), 796–803.

(54) Boswell, C. A.; Lei, X. C.; Schweiger, M.; Reich, M.; Ferl, G. Z.; Theil, F.; Fielder, P. J.; Khawli, L. A. In vivo antibody uptake and physiological measurements in mouse lung and muscle: A compartmental physiologically-based pharmacokinetic (PBPK) modeling approach. *J. Labelled Compd. Radiopharm.* **2009**, *52*, S102–S102.

blood from donor mice into study mice. Lower uptake of ^{99m}Tc in liver, kidney, gut, heart, and fat for the indirect method relative to direct RBC labeling was demonstrated by invasive tissue distribution; reduced renal clearance and an overall decrease in whole-body background was confirmed by SPECT-CT imaging. Furthermore, a previously reported PBPK model demonstrated sizable differences in cumulative tissue uptake of an antibody when using literature versus measured V_v values, demonstrating the importance of obtaining accurate values for physiological parameters. Taken together, these observations suggest that this novel indirect RBC labeling method may ultimately benefit PBPK modeling efforts by providing more accurate measurements of vascular volume than the direct in vivo method, especially in organs involved in probe clearance.

Acknowledgment. The authors would like to thank Jose Imperio, Kirsten Messick, Nicole Valle, and Shannon Stainton for excellent animal studies support. They also express appreciation to Daniela Bumbaca, Saritha Goriparthi, Ruedi Port, Lu Xu, Simon Williams, Nicholas Lewin-Koh, Priyanka Gupta, Saileta Prabhu, Dan Lu, and Yi Zhang for helpful discussions. Guidance and support for small animal imaging was kindly provided by JoAnn Zhang and Sam Kislevitz. Apologies are extended to those whose important and relevant work was omitted due to lack of space. All authors are employees of Genentech, a member of the Roche Group, and hold financial interest in Roche.

MP100183K